Technical Reference on Hydrogen Compatibility of Materials

Austenitc Steels:
300-Series Stainless Alloys
Stabilized Alloys, Types 321 and 347 (code 2104)

Prepared by:

B.P. Somerday, Sandia National Laboratories, Livermore CA

Editors
C. San Marchi
B.P. Somerday
Sandia National Laboratories

This report may be updated and revised periodically in response to the needs of the technical community; up-to-date versions can be requested from the editors at the address given below or downloaded at http://www.ca.sandia.gov/matlsTechRef/ . The content of this report will also be incorporated into a Sandia National Laboratory report (SAND2008-1163); the most recent version can be obtained from the link above. The success of this reference depends upon feedback from the technical community; please forward your comments, suggestions, criticisms and relevant public-domain data to the authors C. San Marchi (cwsanma@sandia.gov) and/or B.P. Somerday (bpsomer@sandia.gov) at:

Sandia National Laboratories
Technical Reference on Hydrogen Compatibility of Materials
MS-9404
7011 East Ave
Livermore CA 94550.

This document was prepared with financial support from the Safety, Codes and Standards program element of the Hydrogen, Fuel Cells and Infrastructure program, Office of Energy Efficiency and Renewable Energy. Sandia is a multiprogram laboratory operated by Sandia Corporation, a Lockheed Martin Company, for the United States Department of Energy under contract DE-AC04-94AL85000.

Sandia National Laboratories

12/15/2008

This page intentionally left blank.

Technical Reference on Hydrogen Compatibility of Materials

Austenitic Steels:

300-Series Stainless Steels,

Stabilized Alloys: Types 321 & 347 (code 2104)

1. General

Types 321 and 347 stainless steels are designed to be single-phase austenite having chromium and nickel contents similar to Types 304 and 316 stainless steels. The alloy chemistries of Types 321 and 347 are distinguished from the other 300-series stainless steels by the addition of titanium (Type 321) or niobium (Type 347). Titanium and niobium are strong carbide formers, and these alloying elements are added to promote the precipitation of intragranular titanium carbides or niobium carbides in preference to intergranular chromium carbides, i.e., $Cr_{23}C_6$. The formation of intergranular chromium carbides in 300-series stainless steels at elevated temperatures is the well-known sensitization phenomenon, which renders grain boundaries more susceptible to corrosion. The Types 321 and 347 stainless steels are referred to as "stabilized" grades because the precipitation of titanium carbides or niobium carbides inhibits sensitization.

The predominant metallurgical variable governing hydrogen-assisted fracture in 300-series stainless steels is alloy composition, particularly nickel content. Results consistently demonstrate that these steels become more susceptible to hydrogen-assisted fracture as nickel content decreases [1-3]. Lower nickel content promotes both strain-induced martensite formation and more severe localized deformation, and both of these metallurgical features have been associated with hydrogen-assisted fracture in 300-series stainless steels. The specifications for nickel in Types 321 and 347 stainless steels are 9-12 wt% and 9-13 wt%, respectively. Based on these specifications, the Types 321 and 347 alloys are expected to be susceptible to hydrogen-assisted fracture when exposed to hydrogen gas, particularly when nickel is at the lower end of the specification.

The limited mechanical property data presented for Types 321 and 347 stainless steels in this chapter suggest that these alloys can be susceptible to hydrogen-assisted fracture, however not all data indicate such susceptibility. The inconsistency in the hydrogen-assisted fracture response reflected by the data may be attributed to materials testing variables, such as loading rate and the method of hydrogen exposure.

1.1 Composition and microstructure

Table 1.1.1 provides the alloy composition specifications for Types 321 and 347 stainless steels. Table 1.1.2 summarizes the alloy compositions and product forms of the Types 321 and 347 stainless steels used in hydrogen compatibility studies that are cited in this chapter.

1.2 Common designations

Type 321: UNS32100 (321), UNS32109 (321H)

Type 347: UNS34700 (347), UNS34709 (347H), UNS34751 (347LN)

2. Permeability, Diffusivity and Solubility

References [1, 4, 5] provide summaries of permeability, diffusivity, and solubility data for hydrogen in austenitic stainless steels. The permeability, diffusivity, and solubility *vs* temperature relationships for 300-series stainless steels are clustered in a band, which includes relationships for Types 321 and 347 stainless steels [1, 5]. The parameters in selected permeability (Φ), diffusivity (D), and solubility (S) relationships for Types 321 and 347 stainless steels are listed in Table 2.1. Also included in Table 2.1 are parameters for relationships that are expected to provide reasonable approximations for all 300-series stainless steels.

3. Mechanical Properties: Effects of Gaseous Hydrogen

3.1 Tensile properties

3.1.1 Smooth tensile properties

Tensile fracture data from smooth specimens strained in high-pressure hydrogen gas demonstrate that Types 321 and 347 stainless steels can be susceptible to hydrogen-assisted fracture, but results are not consistent. Tensile data measured at room temperature are summarized in Table 3.1.1.1. Data for a Type 347 stainless steel (material L72) reveal that testing in 69 MPa hydrogen gas severely degrades ductility, where the reduction in area (RA) in hydrogen is less than 50% of the value in helium. Data for a Type 321 stainless steel (material W73) reveal a more moderate effect of hydrogen on ductility. In this case, the RA measured in 34.5 MPa hydrogen gas was only about 10% less than the value measured in helium. Two possible variables that could account for the difference in the effect of hydrogen on these two materials are the hydrogen gas pressures and alloy compositions; however, a possible effect of alloy composition (in particular nickel content) cannot be assessed since this information was not provided for Type 347 material L72.

A more notable discrepancy in susceptibility to hydrogen-assisted fracture is found for the two Type 347 materials in Table 3.1.1.1. While testing in hydrogen gas causes a reduction in ductility greater than 50% for material L72, hydrogen has no effect on ductility for material H73. Although the hydrogen gas pressures are different for the two materials, both pressures are high enough to cause hydrogen-assisted fracture in 300-series stainless steels. Two other possible sources for the difference in hydrogen-assisted fracture behavior are the alloy compositions and tensile strain rates. Higher strain rates are known to mitigate environment-assisted fracture when straining and environmental exposure are conducted concurrently. The strain rate used during testing of material H73 is relatively high and could mitigate hydrogen-assisted fracture, since the combination of short test duration and low hydrogen diffusivity may limit hydrogen uptake into the material.

Tensile properties measured at low and elevated temperatures are summarized in Tables 3.1.1.2 and 3.1.1.3. A general trend for austenitic stainless steels is that hydrogen effects on

ductility are minimized at low temperature (i.e., < 150 K) and elevated temperature (i.e., > 300 K) and are greatest at a temperature near 200 K [1, 6]. The effect of hydrogen on ductility for the Type 321 steel is similar at room temperature and 144 K; in both cases, the RA measured in hydrogen is about 10-15% less than the value measured in helium. It is possible that hydrogen-assisted fracture would be more pronounced at a temperature near 200 K. For the Type 347 material H73, ductility is not affected by hydrogen gas at 111 K or 950 K. Although these trends for the Type 347 steel may be consistent with expected temperature effects, the high tensile strain rate must be considered in this case.

3.1.2 Notched tensile properties

Results from tests in high-pressure hydrogen gas indicate that hydrogen-assisted fracture may be more severe in notched tensile specimens. The data for Type 321 material W73 strained in 34.5 MPa hydrogen gas at room temperature (Table 3.1.2.1) show that RA is severely degraded (>60% loss in RA) and strength is also reduced (>10% loss in σ_s). These effects of hydrogen on tensile properties are more pronounced compared to results from smooth specimens of Type 321 material W73 (Table 3.1.1.1). The tensile properties for Type 347 material H73 are not affected by hydrogen at room temperature; however, the displacement rate for these tests was relatively high and could have mitigated hydrogen-assisted fracture.

Properties measured from notched tensile specimens at low and elevated temperatures are summarized in Tables 3.1.2.2 and 3.1.2.3. Hydrogen did not affect the tensile properties of Type 321 material W73 at 144 K. This tensile behavior at 144 K is generally consistent with the expectation that hydrogen has a diminished effect on ductility for austenitic stainless steels in the temperature range 100-150 K. The tensile properties of Type 347 material H73 were not significantly affected by hydrogen at either 111 K or 950 K. This trend is consistent with expected temperature effects, but the high displacement rates that were employed in the study of Type 347 [7] must also be considered.

3.2 Fracture mechanics

3.2.1 Fracture toughness

Fracture toughness tests were conducted on Types 321 and 347 stainless steels in 34.5 MPa hydrogen gas [7, 8]. The measurements were conducted using linear elastic fracture mechanics methods; however, these test methods are not appropriate for low-strength, high-toughness materials such as the austenitic stainless steels. Consequently, the test methods and material property data are considered to be not reliable.

3.2.2 Threshold stress intensity factor

Tests to measure the threshold stress intensity factor were conducted for Type 321 stainless steel in 34.5 MPa hydrogen gas [8]. The reported test methods and material property data are considered to be not reliable.

3.3 Fatigue

3.3.1 Low-cycle fatigue

Low-cycle fatigue tests conducted on a Type 347 stainless steel did not reveal a detrimental effect of hydrogen. Smooth, uniaxial specimens from the Type 347 material H73 (Table 1.1.2)

were subjected to tension-compression loading (constant total strain range, where the minimum strain was zero) at a frequency of about 0.06 Hz while exposed to 34.5 MPa hydrogen gas. The strain range *vs* number of cycles to failure data are presented in Figure 3.3.1.1. The strain range *vs* number of cycles to failure data from tests in hydrogen gas and helium gas fall on the same trend line.

3.3.2 High-cycle fatigue

The high-cycle fatigue response of Type 347 stainless steel (material H73) was not affected by hydrogen. Stress-controlled, tension-tension tests were conducted in 34.5 MPa hydrogen gas at a frequency of 20 Hz and a load ratio of 0.1 using smooth, uniaxial specimens. The maximum applied tensile stress *vs* number of cycles to failure data are presented in Figure 3.3.2.1. The tensile stress *vs* number of cycles to failure data from tests in hydrogen gas and helium gas follow the same trend line, but, as discussed in previous sections, the high frequency (i.e., rate) must be considered when interpreting these results.

3.4 Creep

Tests on Type 347 stainless steel did not reveal an effect of hydrogen on creep rupture life. However, the strain to failure during creep was significantly reduced by hydrogen. Smooth specimens of Type 347 material H73 (Table 1.1.2) were subjected to constant applied load in 34.5 MPa hydrogen gas at 950 K. The time to reach various creep strain levels, time to rupture, and strain to failure were measured as a function of applied stress. These data are summarized in Table 3.4.1, and the stress *vs* time to rupture data are plotted in Figure 3.4.1. The limited data show that at a fixed stress level of about 140 MPa the time to rupture was not affected by hydrogen, but the RA measured after testing in hydrogen gas was about 70% lower than the value measured after testing in helium gas.

3.5 Impact

No known published data in hydrogen gas.

3.6 Disk rupture testing

No known published data in hydrogen gas.

4. Fabrication

4.1 Properties of welds

No known published data in hydrogen gas.

5. References

1. GR Caskey. Hydrogen Effects in Stainless Steels. in: RA Oriani, JP Hirth and M Smialowski, editors. Hydrogen Degradation of Ferrous Alloys. Park Ridge NJ: Noyes Publications (1985) p. 822-862.
2. S Fukuyama, M Imade and K Yokogawa. Development of New Material Testing Apparatus in High-Pressure Hydrogen and Evaluation of Hydrogen Gas Embrittlement of Metals. 2007.

3. C SanMarchi, BP Somerday, X Tang and GH Schiroky. Effects of Alloy Composition and Strain Hardening on Tensile Fracture of Hydrogen-Precharged Type 316 Stainless Steels. International Journal of Hydrogen Energy 33 (2008) 889-904.
4. C San Marchi, BP Somerday and SL Robinson. Permeability, Solubility and Diffusivity of Hydrogen Isotopes in Stainless Steels at High Gas Pressure. Int J Hydrogen Energy 32 (2007) 100-116.
5. XK Sun, J Xu and YY Li. Hydrogen Permeation Behaviour in Austenitic Stainless Steels. Mater Sci Eng A114 (1989) 179-187.
6. L Zhang, M Wen, M Imade, S Fukuyama and K Yokogawa. Effect of Nickel Equivalent on Hydrogen Gas Embrittlement of Austenitic Stainless Steels Based on Type 316 at Low Temperatures. Acta Materialia 56 (2008) 3414-3421.
7. JA Harris and MC VanWanderham. Properties of Materials in High Pressure Hydrogen at Cryogenic, Room, and Elevated Temperatures: Annual Report. Pratt & Whitney Aircraft (NASA contract NAS8-26191), West Palm Beach, FL (1971).
8. RJ Walter and WT Chandler. Influence of Gaseous Hydrogen on Metals: Final Report. Rocketdyne (NASA contract NAS8-25579), Canoga Park, CA (1973).
9. ASTM. ASTM DS-56H, Metals and Alloys in the UNIFIED NUMBERING SYSTEM (SAE HS-1086 OCT01). 2001.
10. JA Harris and MC VanWanderham. Properties of Materials in High Pressure Hydrogen at Cryogenic, Room, and Elevated Temperatures: Final Report. Pratt & Whitney Aircraft (NASA contract NAS8-26191), West Palm Beach, FL (1973).
11. XK Sun, J Xu and YY Li. Hydrogen permeation behavior in metastable austenitic stainless steels 321 and 304. Acta Metall 37 (1989) 2171-2176.
12. EH Van Deventer and VA Maroni. Hydrogen Permeation Characteristics of some Austenitic and Nickel-base Alloys. J Nucl Mater 92 (1980) 103-111.
13. MR Louthan and G Caskey. Hydrogen Transport and Embrittlement in Structural Metals. Int J Hydrogen Energy 1 (1976) 291-305.
14. MR Louthan, GR Caskey, JA Donovan and DE Rawl. Hydrogen Embrittlement of Metals. Mater Sci Eng 10 (1972) 357-368.

Table 1.1.1. Allowable composition ranges (wt%) for Types 321 and 347 stainless steels [9].

UNS No.	AISI No.	Fe	Cr	Ni	Mn	Nb	Ti	Si	C	other
S32100	321	Bal	17.00 19.00	9.00 12.00	2.00 max	—	5xC min	1.00 max	0.08 max	0.030 max S; 0.045 max P
S34700	347	Bal	17.00 19.00	9.00 13.00	2.00 max	10xC min	—	1.00 max	0.08 max	0.030 max S; 0.045 max P

Table 1.1.2. Compositions (wt%) of Types 321 and 347 stainless steels in hydrogen compatibility studies.

Heat	Product Form	Fe	Cr	Ni	Mn	Nb	Ti	Si	C	other	Ref.
S89 321	sheet (A 1223 K/4 h + FC)	Bal	17.96	8.08	0.49	—	0.51	0.84	0.053	0.010 S; 0.032 P	[5]
W73 321	32 mm plate (HR + A)	Bal	17.80	10.45	1.46	—	0.51	0.58	0.06	0.015 S; 0.026 P	[8]
H73 347	19 mm D bar (A 1297 K/1 h + AC + CF)	Bal	18.4	10.10	2.0	0.83*	—	0.94	0.06	0.010 S; P nr	[10]

nr = not reported; A = anneal; AC = air cool; CF = cold finished; D = diameter; FC = furnace cool; HR = hot rolled

* Nb+Ta

Table 2.1. Parameters in permeability, diffusivity and solubility relationships for hydrogen in Types 321 and 347 austenitic stainless steels.

Material	Temperature Range (K)	Pressure Range (MPa)	$\Phi = \Phi_o \exp(-E_\Phi / RT)$		$D = D_o \exp(-E_D / RT)$		$S = S_o \exp(-E_S / RT)$		Ref.
			Φ_o $\left(\frac{\text{mol } H_2}{\text{m} \cdot \text{s} \cdot \text{MPa}^{1/2}}\right)$	E_Φ $\left(\frac{\text{kJ}}{\text{mol}}\right)$	D_o $\left(\frac{\text{m}^2}{\text{s}}\right)$	E_D $\left(\frac{\text{kJ}}{\text{mol}}\right)$	S_o $\left(\frac{\text{mol } H_2}{\text{m}^3 \cdot \text{MPa}^{1/2}}\right)$	E_S $\left(\frac{\text{kJ}}{\text{mol}}\right)$	
S89 321	473-703	0.1	2.44×10^{-4}	62.70	4.61×10^{-7}	53.79	529	8.91	[5, 11]
321 *	497-933	0.6×10^{-6} - 1.2×10^{-2}	8.53×10^{-5}	59.4	—	—	—	—	[12]
347 *	823-973	—	3.59×10^{-4}	69.0	2.55×10^{-6}	61.9	141	7.1	[1]
300-series stainless steels	—	—	1.2×10^{-4}	59.8	8.9×10^{-7}	53.9	135	5.9	[4]

* Alloy composition not reported.

Table 3.1.1.1. Smooth tensile properties of Types 321 and 347 stainless steels tested at room temperature in hydrogen gas. Properties in air and/or helium gas are included for comparison.

Material	Thermal precharging	Test environment	Strain rate (s^{-1})	S_y (MPa)	S_u (MPa)	El_u (%)	El_t (%)	RA (%)	Ref.
W73 321	None	Air	0.067 x10^{-3} *	221	600	—	77	71	[8]
		34.5 MPa He		200	579	—	63	66	
		34.5 MPa H_2		255	593	—	64	60	
H73 347	None	34.5 MPa He	0.67 x10^{-3} *,†	461	695	—	37	70	[7]
		34.5 MPa H_2		455	752	—	40	71	
L72‡ 347	None	69 MPa He	—	206	572	—	60	80	[13, 14]
		69 MPa H_2		200	510	—	38	37	

* Estimated from displacement rate and specimen gauge length.
† Strain rate up to S_y. Strain rate increased to 1.3x10^{-3} s^{-1} between S_y and S_u.
‡ Alloy composition not reported.

Table 3.1.1.2. Smooth tensile properties of Types 321 and 347 stainless steels tested at low temperature in hydrogen gas. Properties in helium gas are included for comparison.

Material	Thermal precharging	Test environment	Temp (K)	Strain rate (s^{-1})	S_y (MPa)	S_u (MPa)	El_u (%)	El_t (%)	RA (%)	Ref.
W73 321	None	34.5 MPa He	144	0.067 x10^{-3} *	—	855	—	48	67	[8]
		34.5 MPa H_2			—	841	—	43	56	
H73 347	None	34.5 MPa He	111	0.67 x10^{-3} *,†	720	1378	—	43	64	[7]
		34.5 MPa H_2			664	1267	—	43	64	

* Estimated from displacement rate and specimen gauge length.
† Strain rate up to S_y. Strain rate increased to 1.3x10^{-3} s^{-1} between S_y and S_u.

Table 3.1.1.3. Smooth tensile properties of Type 347 stainless steel tested at elevated temperature in hydrogen gas. Properties in helium gas are included for comparison.

Material	Thermal precharging	Test environment	Temp. (K)	Strain rate (s^{-1})	S_y (MPa)	S_u (MPa)	El_u (%)	El_t (%)	RA (%)	Ref.
H73 347	None	34.5 MPa He	950	0.67 x10^{-3} *,†	397	414	—	25	67	[7]
		34.5 MPa H_2			397	424	—	25	67	

* Estimated from displacement rate and specimen gauge length.
† Strain rate up to S_y. Strain rate increased to 1.3x10^{-3} s^{-1} between S_y and S_u.

Table 3.1.2.1. Notched tensile properties of Types 321 and 347 stainless steels tested at room temperature in hydrogen gas. Properties in helium gas are included for comparison.

Material	Specimen	Thermal precharging	Test environment	Displ. rate (mm/s)	S_y † (MPa)	σ_s (MPa)	RA (%)	Ref.
W73 321	(a)	None None	34.5 MPa He 34.5 MPa H_2	~0.4 x10^{-3}	200 255	779 683	6.4 2.3	[8]
H73 347	(b)	None None	34.5 MPa He 34.5 MPa H_2	42 x10^{-3}	461 455	1184 1169	20 18	[7]

† yield strength of smooth tensile bar

(a) V-notched specimen: 60˚ included angle; minimum diameter = 3.81 mm; maximum diameter = 7.77 mm; notch root radius = 0.024 mm. Elastic stress concentration factor, K_t = 8.4.

(b) V-notched specimen: 60˚ included angle; minimum diameter = 8.00 mm; maximum diameter = 12.70 mm; notch root radius = 0.051 mm. Elastic stress concentration factor, K_t = 8.4.

Table 3.1.2.2. Notched tensile properties of Types 321 and 347 stainless steels tested at low temperature in hydrogen gas. Properties in helium gas are included for comparison.

Material	Specimen	Thermal precharging	Test environment	Temp. (K)	Displ. rate (mm/s)	S_y † (MPa)	σ_s (MPa)	RA (%)	Ref.
W73 321	(a)	None None	34.5 MPa He 34.5 MPa H_2	144	~0.4 x10^{-3}	— —	986 972	12 12	[8]
H73 347	(b)	None None	34.5 MPa He 34.5 MPa H_2	111	42 x10^{-3}	720 664	1579 1540	12 12	[7]

† yield strength of smooth tensile bar

(a) V-notched specimen: 60˚ included angle; minimum diameter = 3.81 mm; maximum diameter = 7.77 mm; notch root radius = 0.024 mm. Elastic stress concentration factor, K_t = 8.4.

(b) V-notched specimen: 60˚ included angle; minimum diameter = 8.00 mm; maximum diameter = 12.70 mm; notch root radius = 0.051 mm. Elastic stress concentration factor, K_t = 8.4.

Table 3.1.2.3. Notched tensile properties of Type 347 stainless steel tested at elevated temperature in hydrogen gas. Properties in helium gas are included for comparison.

Material	Specimen	Thermal precharging	Test environment	Temp. (K)	Displ. rate (mm/s)	S_y † (MPa)	σ_s (MPa)	RA (%)	Ref.
H73 347	(b)	None	34.5 MPa He	950	42 x10^{-3}	397	713	19	[7]
		None	34.5 MPa H_2			397	693	16	

† yield strength of smooth tensile bar.

(b) V-notched specimen: 60˚ included angle; minimum diameter = 8.00 mm; maximum diameter = 12.70 mm; notch root radius = 0.051 mm. Elastic stress concentration factor, K_t = 8.4.

Table 3.4.1. Creep properties of Type 347 stainless steel tested at 950 K in hydrogen gas. Properties in helium gas are included for comparison.

Material	Stress (MPa)	Test environment	Time to creep (hr)			Time to rupture (hr)	El (%)	RA (%)	Ref.
			0.5%	1.0%	2.0%				
H73 347	279	34.5 MPa He	<0.1	0.15	0.2	0.3	8.7	48	[7]
	134	34.5 MPa He	3.0	9.0	16.5	24.5	8.5	44	
	137	34.5 MPa H_2	8.0	14.0	21.0	23.9	2.6	14	
	81	34.5 MPa H_2	60.0	115.0	187.0	>187.0	NCR	NCR	

NCR = no creep rupture

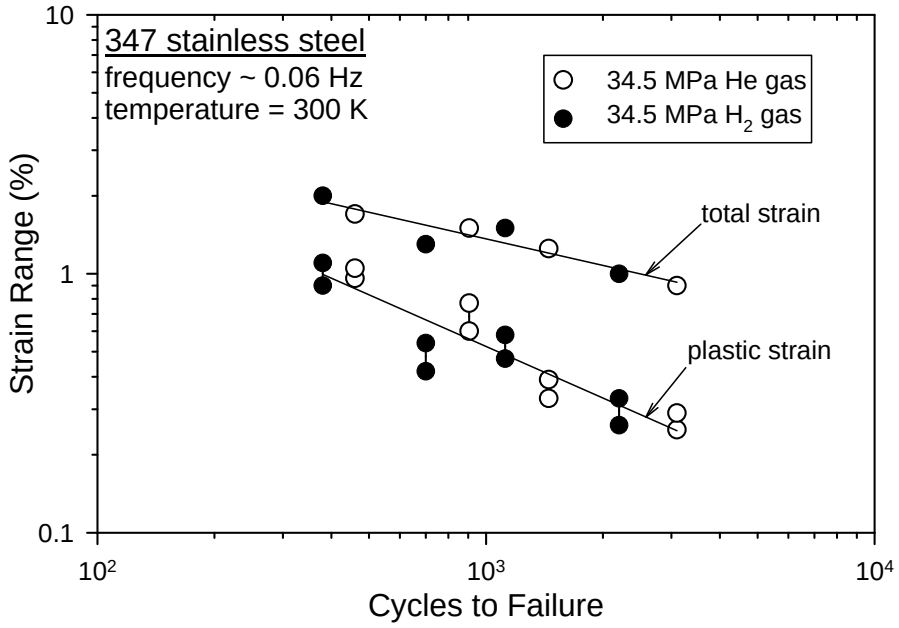

Figure 3.3.1.1. Applied strain range *vs* number of cycles to failure data for Type 347 stainless steel (material H73) [7]. Two plots are presented for one set of results: the data are plotted using the plastic strain range as well as the total strain (elastic + plastic) range. Two symbols are plotted for each data point on the plastic strain range plot, where the symbols indicate the variation in plastic strain during the test. Data are shown for tests conducted in both hydrogen gas and helium gas.

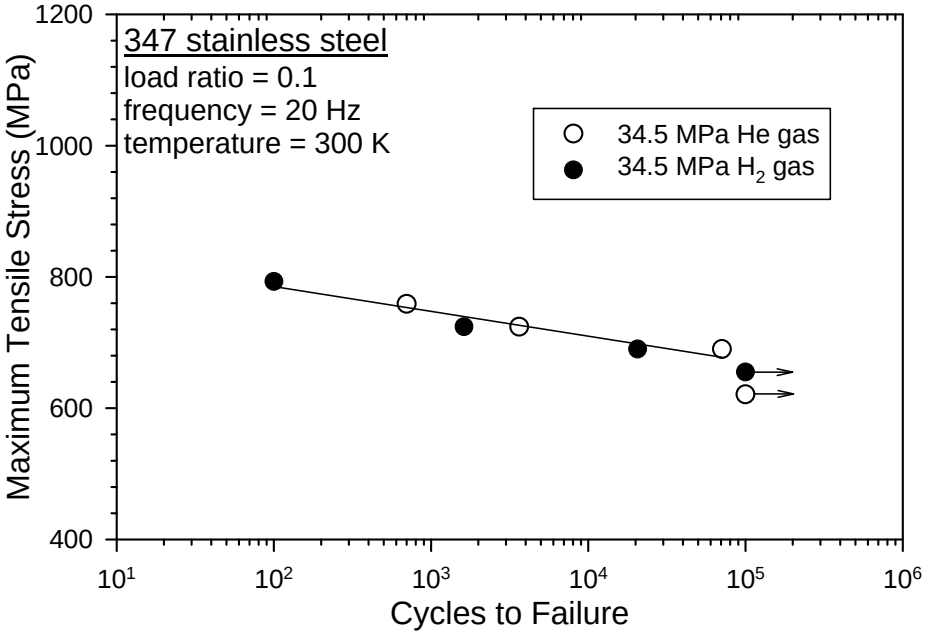

Figure 3.3.2.1. Maximum tensile stress *vs* number of cycles to failure data for Type 347 stainless steel (material H73) [7]. Data are shown for tests conducted in both hydrogen gas and helium gas. The test specimens at the two lowest stress levels did not fail and tests were terminated at 10^5 cycles.

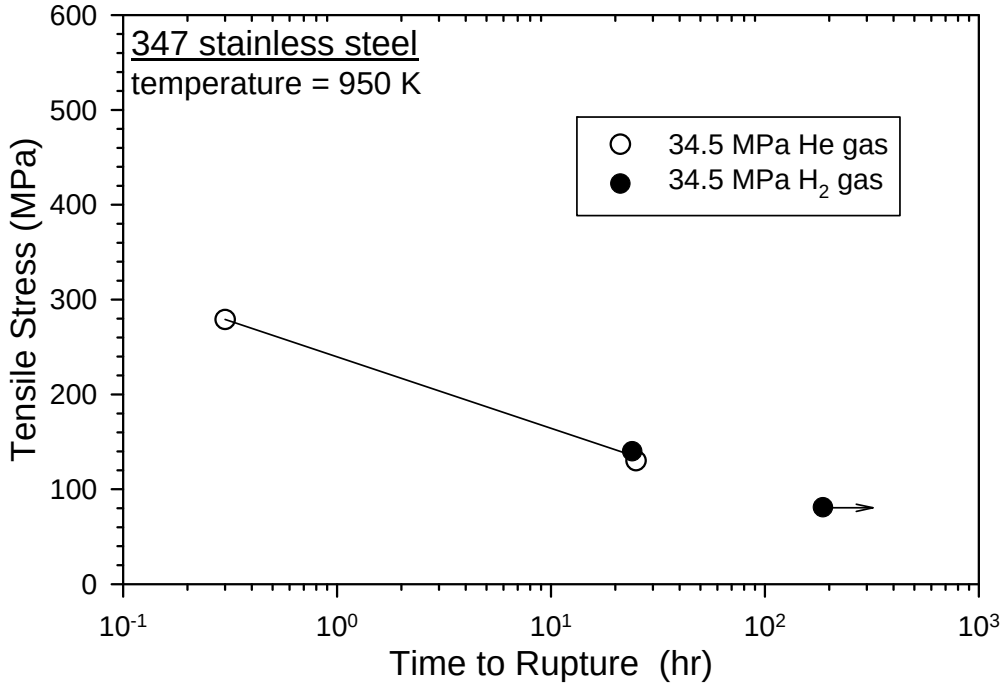

Figure 3.4.1. Tensile stress *vs* time to rupture data for Type 347 stainless steel (material H73) [7]. Data are shown for tests conducted in both hydrogen gas and helium gas. The test specimen at the lowest stress level did not fail and the test was terminated at about 200 hr.